LEVEL II

A KINETIC STUDY OF THE REACTION OF CH_3O_2 WITH NO_2

by

A. R. Ravishankara
F. L. Eisele
P. H. Wine

DTIC
ELECTE
NOV 0 3 1980
S   D
E

Prepared for:

GEORGIA INSTITUTE OF TECHNOLOGY

Engineering Experiment Station
Atlanta, Georgia 30332

GT EES

80 10 30 004

(18) (19) 80-38-VOL-1

1. Report No.	2. Government Accession No.	3. Recipient's Catalog No.
FAA/EE 80-38, vol. 1	AD-A091293	(11)

4. Title and Subtitle	5. Report Date
A Kinetic Study of the Reaction of CH_3O_2 with NO_2. (6) Volume I,	1980
	6. Performing Organization Code

7. Author(s)	8. Performing Organization Report No.
(10) A.R. Ravishankara, R.L. Eisele, P.H. Wine	

9. Performing Organization Name and Address	10. Work Unit No. (TRAIS)
Engineering Experiment Station Georgia Institute of Technology Atlanta, Georgia 30332	
	11. Contract or Grant No. (15) DOT-FA78WA-4259
	13. Type of Report and Period Covered

12. Sponsoring Agency Name and Address	
U. S. Department of Transportation Federal Aviation Administration 800 Independence Ave., S. W. Washington, D. C. 20591	14. Sponsoring Agency Code

15. Supplementary Notes

(12) 39

16. Abstract

17. Key Words	18. Distribution Statement
	This document is available to the public through the National Technical Information Service, Springfield, Va. 22161

19. Security Classif. (of this report)	20. Security Classif. (of this page)	21. No. of Pages	22. Price
Unclassified	Unclassified	38	

153850

A KINETIC STUDY OF THE REACTION OF

CH_3O_2 WITH NO_2

Contract #DOT-FA78WA-4259

Report # FAA-EE-80-38

VOLUME I

Submitted to:

U.S. Department of Transportation
Federal Aviation Administration
800 Independence Avenue, S.W.
Washington, D.C.   20591

by

Molecular Sciences Group
Electromagnetics Laboratory
Engineering Experiment Station
Georgia Institute of Technology
Atlanta, Georgia   30332

Contracting through;

Georgia Tech Research Institute
Georgia Institute of Technology
Atlanta, Georgia   30332

Prepared by:

A.R. Ravishankara
F.L. Eisele
P.H. Wine

ABSTRACT

The technique of pulsed laser photolysis-long path laser absorption is employed to study the kinetics of the reaction $CH_3O_2 + NO_2 + N_2 \xrightarrow{k_1}$ $CH_3O_2NO_2 + N_2$ over the temperature range 253-353 K. At all temperatures, k_1 is found to monotonically increase with increasing N_2 pressure over the range 76-722 torr, indicating that reaction occurs predominantly by addition. The dependence of k_1 on N_2 pressure shows that the reaction is in the fall-off region between second and third order kinetics. These results are compared with previous results and their atmospheric implications are discussed.

TABLE OF CONTENTS

Introduction

The methylperoxy radical is an important intermediate in reaction sequences through which hydrocarbons are oxidized in both atmospheric and combustion processes. In combustion systems the fate of peroxy radicals is predominantly governed by their reactions with other radicals, while in the atmosphere, and particularly in the polluted troposphere, it is expected that reactions with stable molecules will be important. The major species which can react with CH_3O_2 in the atmosphere include HO_2, NO, NO_2, SO_2, and O_3. The rate constant for the reaction of CH_3O_2 with NO has been recently measured using direct kinetic techniques[1-3] and found to be nearly as fast as the reaction of HO_2 with NO.[4,5] Therefore, in a polluted atmosphere where NO_x concentrations are high, methyl peroxy radicals are expected to react mostly with NO_x species. For the subject reaction of the present investigation,

$$CH_3O_2 + NO_2 + N_2 \xrightarrow{k_1} CH_3O_2NO_2 + N_2 \qquad (1)$$
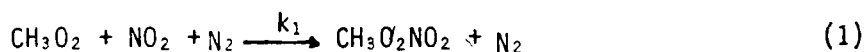
to effectively compete with the reaction of CH_3O_2 with NO,

$$CH_3O_2 + NO \xrightarrow{k_2} CH_3O + NO_2 \qquad (2)$$

the value of k_1 should be of similar magnitude as that of k_2. If Reaction (1) were a significant path for CH_3O_2 removal, NO_2 production (and the subsequent O_3 generation) would be reduced.

Until recently most rate coefficients for CH_3O_2 radical reactions were obtained by steady state competitive experiments.[6-8] In the past few years direct measurement techniques such as discharge flow-mass spectrometry, flash photolysis-ultraviolet absorption, and molecular

modulation-UV absorption spectroscopy have been adopted for CH_3O_2 radical studies.

To date three direct measurements of k_1 have been carried out. Cox and Tyndall[9] utilized the molecular modulation-UV absorption technique and obtained a value of k_1 which was essentially independent of bath gas pressure. The flash photolysis-UV absorption method has been employed by Adachi and Basco,[10] and Sander and Watson[2] to measure k_1. Adachi and Basco's results are in agreement with those of Cox and Tyndall. However, unlike the previous two measurements, Sander and Watson found Reaction (1) to be pressure dependent. These investigators carried out their experiments under secondary reaction free conditions using a very sensitive probe for CH_3O_2 radicals. Hence, their results appear to be more reliable. There are no previous measurements of k_1 as a function of temperature.

In the present study, k_1 was measured as a function of N_2 diluent gas pressure and temperature using the recently developed technique of pulsed laser photolysis-long path laser absorption. Due to the monochrmoaticity of the photolysis laser, and the resultant photolysis specificity, all unwanted photofragments were essentially eliminated, while the high intensity of the CW 257 nm probing laser beam enabled measurement of very low concentrations of CH_3O_2. Under these secondary reaction free conditions, our measured value of k_1 was found to be pressure dependent in excellent agreement with Sander and Watson. Also, as to be expected for an addition reaction, k_1 was found to increase with decreasing temperature.

The technique of pulsed laser photolysis-laser induced fluorescence was originally proposed to be employed in the study of Reaction (1). CH_3O_2 radicals were to be produced using either 355 nm photolysis of $Cl_2/CH_4/O_2$ mixtures or UV photolysis of azomethane. To follow the course of the reaction either NO_2 reactant in excess CH_3O_2 or CH_2O product in excess NO_2 were to be monitored using laser induced fluorescence.

There were two developments which excluded carrying out laser induced fluorescence detection of CH_2O to map out the course of Reaction (1): a) we could not obtain the expected 10 mW of UV laser output in the intracavity Ar^+ laser pumped tunable dye laser (in fact, we succeeded in obtaining only 20 μW!), and b) in some recent studies it was shown that Reaction (1) proceeds predominantly through an addition mechanism; therefore, the CH_2O product yield is very low, and an unrealistically high detection sensitivity for CH_2O would be needed. For these reasons, we abandoned the idea of monitoring CH_2O.

The second approach of following the NO_2 decay in excess CH_3O_2 was pursued when the first approach failed. The primary requirement for this experiment was the creation of a uniform known concentration of CH_3O_2 by laser photolysis. We have succeeded in obtaining a spatially uniform, 'top hat' profiled laser beam using a segmented aperture optical integrator. With this added capability, we can produce CH_3O_2 radicals in excess over NO_2. Our capability to detect NO_2 via laser induced fluorescence (pumped by the 488 nm output of an argon ion laser) is well developed and has been used in the study of the reaction of CH_3O_2 with NO.[3] However, when we tried to monitor NO_2 in excess CH_3O_2, we found the decay of NO_2 to be non-exponential. The decay rates decreased with time due to the disproportionation reaction,

3

$$CH_3O_2 + CH_3O_2 \longrightarrow Products \; . \qquad\qquad (a)$$

The rate coefficient for Reaction (a) is reasonably well known.[2] A simple calculation shows that unless Reaction (1) is very fast, i.e., is $\sim 1 \times 10^{-11}$ $cm^3 molecule^{-1} s^{-1}$, the CH_3O_2 concentration would decrease by more than 10% by the time the NO_2 concentration dropped to 1/e times its original value. Therefore, it was evident that even though we could measure k_1 at low temperatures and high pressures the required range of pressures and temperatures could not be covered.

Upon realizing that our originally proposed methods would be either inapplicable or of limited use, we decided to develop the laser photolysis-long path laser absorption technique. This effort was very successful and we completed the measurement of k_1 as a function of temperature and pressure, as discussed below.

PULSED LASER PHOTOLYSIS-LONG PATH LASER ABSORPTION KINETICS

STUDY OF THE REACTION OF METHYLPEROXY RADICALS WITH NO_2

Experimental

A schematic diagram of the apparatus used to study Reaction (1) is shown in Figure 1. A jacketed reactor with an internal volume of $\sim$ 1ℓ and a length of 107 cm was constructed out of pyrex. The cell was maintained at a constant temperature by circulating either methanol (253-298 K) or ethylene glycol (298-353 K) from a temperature controlled circulator through the outer jacket. It was found that the temperature was uniform to within 2°C throughout the length of the cell. On both ends of the reactor two 1/8" thick, 2" diameter quartz (Suprasil 1) plates were attached using O-ring seals and metal clamps. The reactants were pre-mixed in a mixing chamber and slowly flowed through the reactor. At the outlet of the reactor, the pressure in the system was measured using an absolute one-turn Bourdon gauge (Wallace and Tiernan Model FA160-NN) before the gas mixture was pumped out.

Azomethane/N_2 and NO_2/N_2 mixtures were prepared in 12ℓ bulbs on a gas handling system. The bulbs were connected to the mixing chamber using teflon tubing and stainless steel ultra-torr fittings. The rates of flow of the azomethane/N_2 mixture, NO_2/N_2 mixture, N_2, and O_2 into the mixing chamber were controlled by stainless steel needle valves and measured by calibrated mass flow transducers. The tubes leading into the mixing chamber had radial outlets to turbulently mix the gases. The concentration of each component in the reaction mixture was determined from measurements of appropriate mass flow rates and the total pressure. The concentration of NO_2 in the NO_2/diluent mixture was checked (before and after each set of experiments) by simultaneous measurements of the total pressure (of the mixture) and NO_2 absorption

6
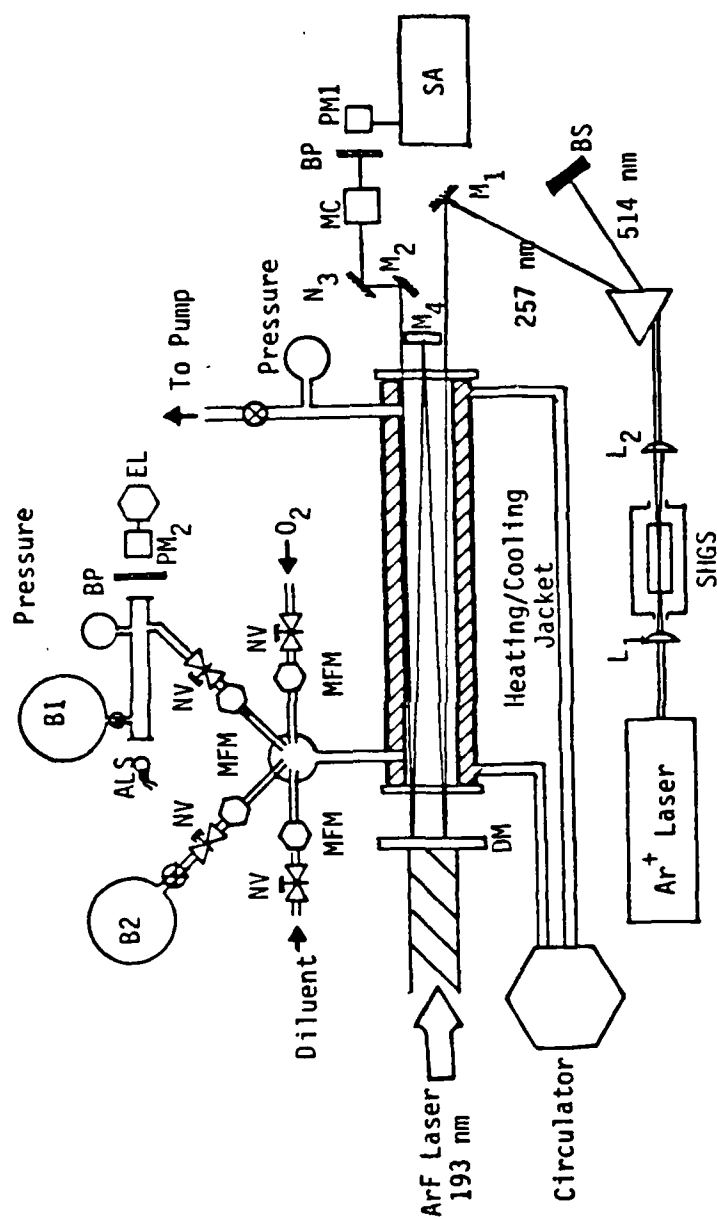
Figure 1. A Schematic Diagram of Pulsed Laser Photolysis-Long Path Laser Absorption Apparatus.

at 366 nm. The measurements were carried out using an Hg pen-ray lamp as the light source, a 70 cm absorption cell, and a bandpass filter-photo-multiplier detector combination. The absorption cross section used to determine [NO_2], 5.75×10^{-10} cm^2,[11] has been previously measured in our laboratory and agrees well with the literature value.[12] The azomethane concentration was occasionally checked by a method identical to that for NO_2; the absorption cross section of azomethane was measured to be 1.13×10^{-20} cm^2 at 366 nm, which is slightly higher than the published value,[13] but in agreement with other recent measurements.[14]

Azomethane was prepared as described in Appendix I. NO_2, obtained from Matheson Gas Products, had a stated purity of 99.5%, and was purified by mixing it with UHP O_2 to convert all NO to NO_2, and subsequently sub-jecting it to freeze-pump-thaw cycles to remove O_2. NO_2 and O_2 were Matheson grade and had stated purity levels of 99.9995% and 99.99%, respectively; these gases were used as supplied.

An ArF excimer laser, the photolysis light source, was housed in an adjoining room, approximately 2 meters from the front window of the reactor. We found this spatial separation to be essential if a uniform beam was to be obtained. (Operation of the laser under slightly fluorine-rich conditions also helped to make the beam more diffuse.) The beam was approximately 2 cm x 7 cm by the time it reached the reactor. The laser beam was transmitted through a custom made dielectric mirror, DM and traveled through the reactor impinging on the MgF_2 coated aluminum mirror M_4 where a fraction of the beam was reflected back into the reactor. Both mirrors DM and M_4 were mounted on precision mirror mounts with vernier control to enable very fine adjustments. (DM was specially coated for us by Acton Research Corp. to have $\sim$ 85% transmisstion at 193 nm and $\geq$ 95% reflectivity at 257 nm.)

8

The doubled CW 257 nm UV beam was generated as described in Appendix II. This beam was diverted into the reactor using mirror M_1 so as to traverse the volume photolyzed by the ArF laser beam. By adjusting Mirrors DM and M_4, the CW UV beam was multipassed 8 times through the reactor to obtain a path length of $\sim$ 860 cm. The 8th pass was diverted away from the reactor by a small aluminum mirror M_2, passed through a methanol cell and a 257 nm bandpass filter, and detected by a quartz envelope 1P28 (PCA) photomultiplier tube. (It was necessary to use a methanol filter to prevent the 193 nm laser pulse from being detected by the PM tube.) The output of the PM tube was amplified and stored in a signal averager (Tracor-Northern 1500) operating in the analog mode and triggered 150 μsec after the photolysis pulse. (We could not obtain a usable signal in the first 150 μsec due to interference from fluorescence induced by the 193 nm beam.) The PM tube was operated at $\sim$ 600 V to have a resistor bridge current of $\sim$ 1 mA. The anode current was always kept below 1 μA by using suitable neutral density filters to reduce the intensity of the 257 nm beam. To increase the signal-to-noise ratio of the decay curves, 16 to 64 flashes were averaged. The pulse rate of the photolysis laser (0.03 to 0.01 Hz) was such that the contents of the reactor was replaced between consecutive photolysis pulses. This was necessary in order to sweep out the products (which also absorb the probing beam) and use identical gas mixtures for each flash. In preliminary experiments it was established that as long as the cell was swept out between flashes either the laser repetition rate or the flow rate of the mixture through the reactor did not affect the measured value of k_1. The intensity of the transmitted 257 nm beam before photolysis was higher than that obtained when all CH_3O_2 had reacted. This residual absorption has been observed by both Cox and

9

Tyndall,[9] and Sander and Watson,[2] and is attributed to the absorption by
$CH_3O_2NO_2$, the product of Reaction (1). Sander and Watson[2] have shown
that the absorption of the analyzing beam by a reaction product which is
stoichiometrically coupled to the monitored reactant species by a single
reaction (as it is in the present case) does not affect the kientic data
that is obtained. In addition, they point out that the proper I_0 value
that should be used in the data analysis is the intensity of the 257 nm
beam when all CH_3O_2 has reacted, and not the value obtained when $CH_3O_2NO_2$
is absent. It is worth noting that since the intensity of the probing
beam was high, the signal-to-noise was excellent and we could easily work
with less than 3% initial absorption and still follow the decay of CH_3O_2
down to $\sim$ 4 1/e times!

Results

Reaction (1) was studied as a function of the pressure of the bath gas N_2 and temperature (at 298K, 76-722 torr; at 353K, 330-696 torr; at 253K, 109-510 torr). As pointed out earlier, all experiments were carried under pseudo-first order conditions with $[NO_2] > [CH_3O_2]$. Figure 2 shows typical decays of $[CH_3O_2]$ as a function of time; the decays are exponential and thus confirm the presence of pseudo-first order conditions. The decay of $[CH_3O_2]$ was usually followed, for 3 1/e times. The pseudo-first order rate constant, k_1' ($\equiv$ slope of $\ln[CH_3O_2]$ vs. t plots) was measured for various values of $[NO_2]$ at each temperature and N_2 pressure. k_1' was then plotted against $[NO_2]$; the slope of this line gave k_1. Figure 3 shows one such plot. It should be pointed out that the fitting procedure we employed (a linear least squares analysis) did not force the k_1' vs. $[NO_2]$ line to a zero intercept; in our system, it is possible to have a non-zero intercept since the entire volume of the reactor was not subjected to the photolysis. The intercepts in all our experiments were small relative to the measured k_1' values.

Table I lists the individual values of k_1' along with all the pertinent experimental conditions. The quoted errors for k_1, calculated from the slope of k_1' vs. $[NO_2]$ plots, are 2σ and reflect the precision of the measurement. The absolute accuracy of the measured values of k_1, is expected to be $\sim 20\%$ which includes the error in the $[NO_2]$ measurement.

Table II lists the values of k_1 obtained at various N_2 pressures and temperatures. Figure 4 shows a plot of k_1 as a function N_2 number density at three different temperatures. The solid lines drawn through these points are visual best fits.
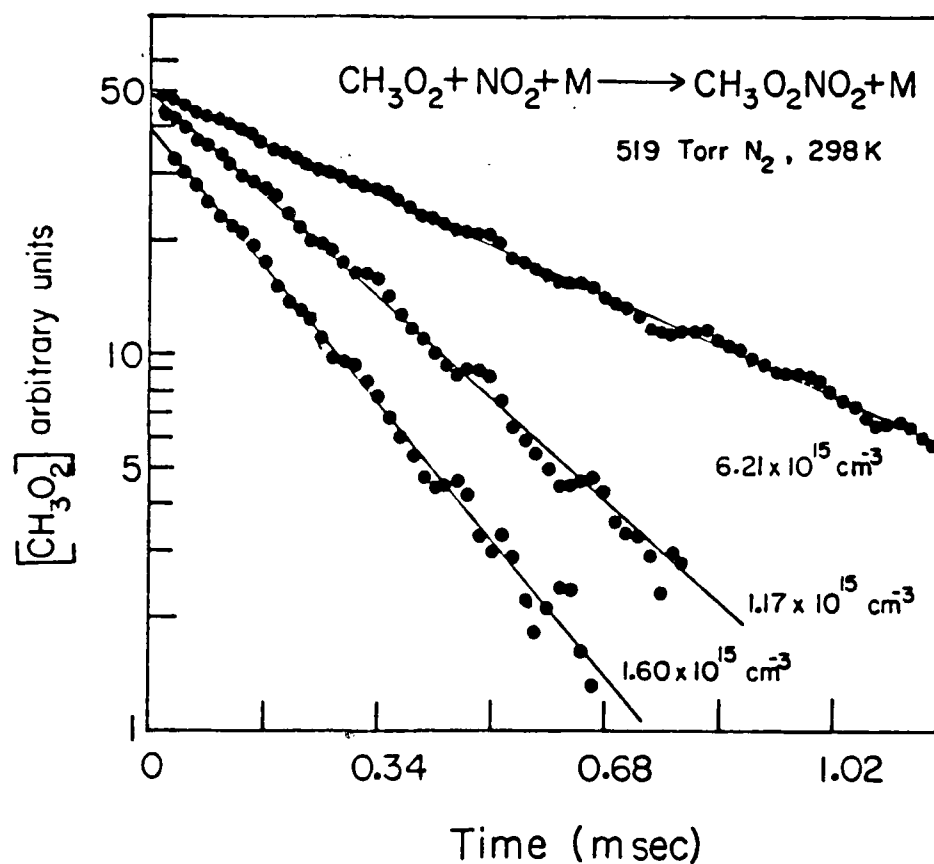
Figure 2. [CH₃O₂] Temporal Profiles in the Presence of Varying
Amounts of NO₂. The concentration of NO₂ for each
decay curve is shown next to the least squares lines
drawn through the experimental points.

12
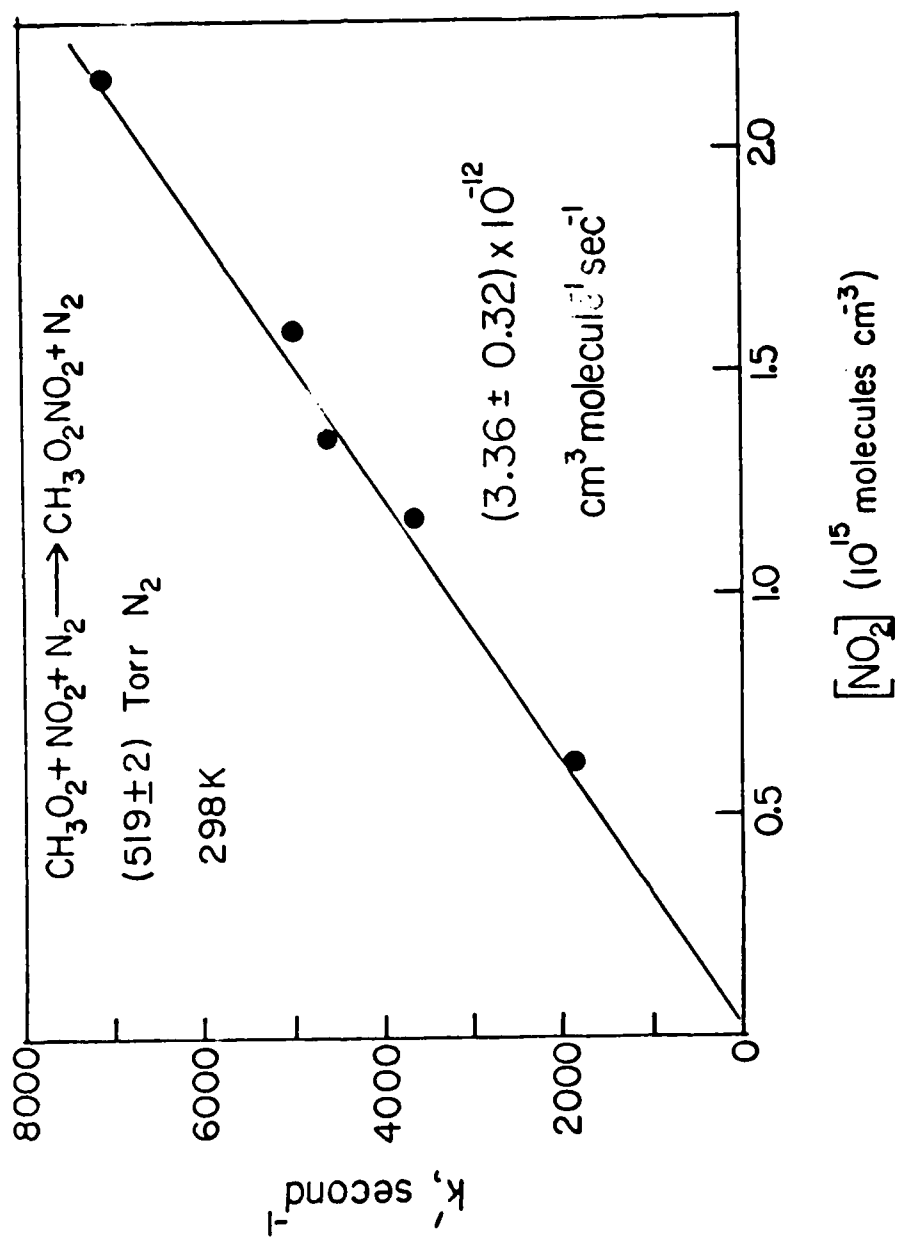
Figure 3. Plot of Pseudo-First Order Rate Constants vs. NO_2 Concentration at 298K and 519 torr of N_2.

13

Table I. Rate Constant Data for the Reaction of CH_3O_2 with NO_2.

Temperature K	N_2 Pressure torr	[Azomethane] 10^{15} cm^{-3}	$[O_2]$ 10^{17} cm^{-3}	$[CH_3O_2]_0$[a] 10^{12} cm^{-3}	$[NO_2]$ 10^{14} cm^{-3}	k_1', $10^3 \times$ s^{-1}	$k_1 \times 10^{12}$[b] cm^{3}molecule^{-1}s^{-1}
298	76±3	0.80	2.70	2.29	6.95	1.15	
		0.78	2.69	1.96	11.73	1.75	
		0.74	2.60	1.31	19.10	2.56	
		0.70	2.63	0.90	24.81	3.64	(1.36±0.23)
	157±2	0.52	4.50	1.13	7.94	1.50	
		1.52	4.34	1.22	10.08	1.70	
		0.53	4.34	1.00	14.96	2.82	
		0.81	4.40	2.33	17.54	3.12	
		0.53	4.47	0.99	21.47	4.05	(1.90±0.32)
	258±3	0.82	3.46	5.60	5.65	1.39	
		0.85	3.50	7.02	12.26	2.90	
		0.79	3.42	6.91	15.60	4.04	
		0.79	3.54	7.00	19.8	5.60	(2.60±0.56)
	352±3	0.77	3.53	2.56	6.87	1.88	
		0.71	3.52	3.39	9.42	2.70	
		0.79	3.52	2.46	11.88	3.70	
		0.67	3.50	2.32	13.63	3.77	
		0.73	3.51	2.66	16.05	4.50	(2.82±0.28)
	519±2	1.14	3.82	2.17	6.21	1.84	
		1.15	3.82	2.85	11.70	3.63	
		1.16	3.78	3.28	13.59	4.57	
		1.23	3.79	3.46	15.95	4.93	
		1.08	3.80	4.80	21.60	7.06	(3.36±0.32)
	722±1	0.821	5.68	3.75	5.38	1.91	
		1.76	5.66	4.00	7.47	2.60	
		0.843	5.68	4.70	9.86	3.42	
		0.88	5.66	5.90	12.79	4.95	
		0.91	5.66	3.20	15.92	6.15	(4.12±0.38)

Temperature K	N_2 Pressure torr	[Azomethane] 10^{15} cm⁻³	$[O_2]$ 10^{17} cm⁻³	$[CH_3O_2]^a$ 10^{13} cm⁻³	$[NO_2]$ 10^{14} cm⁻³	$k\ell$, 10^3 xs⁻¹	k_1 x 10^{12b} cm³ molecule⁻¹ s⁻¹
353	330±3	0.92	3.02	2.98	4.60	0.70	
		0.91	3.50	3.30	9.50	1.38	
		0.93	2.50	1.39	11.81	1.61	
		0.87	2.50	1.70	15.83	2.09	(1.19±0.15)
	354±2	0.96	4.57	2.22	8.64	1.42	
		0.86	4.56	1.97	15.32	2.27	
		1.03	4.56	1.35	24.73	3.81	
		0.79	4.53	1.03	30.21	4.22	(1.35±0.21)
	511±2	1.13	4.18	2.46	7.81	1.78	
		1.36	4.17	3.89	17.44	3.34	
		1.21	4.19	2.18	23.60	4.37	
		1.22	4.16	2.65	28.89	5.41	(1.71±0.10)
	696±2	1.11	4.76	2.23	9.94	2.28	
		2.08	4.69	3.57	20.70	4.17	
		1.74	5.00	3.12	24.12	5.27	
		1.46	4.73	1.71	31.71	6.81	
		1.62	4.73	2.41	4.50	8.84	(1.93±0.20)
253	109±1	1.30	3.60	1.53	2.77	1.05	
		1.39	4.56	1.55	4.02	1.44	
		1.32	3.60	1.62	5.75	2.03	
		1.31	3.70	1.82	7.56	2.36	
		1.31	3.80	0.89	9.16	2.86	
		1.31	3.70	1.31	11.10	3.10	(2.50±0.34)
	250±2	0.57	2.23	1.40	2.61	1.17	
		0.59	2.22	1.62	3.42	1.38	
		0.61	2.22	1.32	5.66	2.29	
		0.61	2.22	1.54	7.89	3.29	
		0.64	2.21	1.60	9.96	3.89	(3.85±0.30)

Temperature K	N_2 Pressure torr	[Azomethane] 10^{15} cm^{-3}	[O_2] 10^{17} cm^{-3}	[CH_3O_2]$_0$[a] 10^{13} cm^{-3}	[NO_2] 10^{14} cm^{-3}	k↓, $10^3 \times$s^{-1}	$k_1 \times 10^{12}$[b] cm^{3}molecule^{-1}s^{-1}
253	503±3	0.60	4.59	1.80	3.00	1.66	
		0.78	5.36	1.30	4.34	2.16	
		0.63	4.56	2.55	6.55	3.01	
		0.62	4.59	2.59	8.52	4.05	(5.10±0.50)
	519	1.11	5.22	2.2	5.85	2.60	
		0.99	5.21	2.6	11.20	5.72	
		0.88	5.21	2.0	18.15	9.72	
		1.10	5.22	2.1	23.8	13.20	(5.8±1.0)

a) The initial concentration of CH_3O_2, [CH_3O_2]$_0$, was calculated by back-extrapolating the decay curve for 150 μsec. (the delay between photolysis and initiation of signal acquisition.)

b) The quoted errors are 2σ and represent the precision of the measurements.

Table II. Rate Constants for the Reaction of CH_3O_2 with NO_2 as a Function of Temperature and N_2 Pressure.

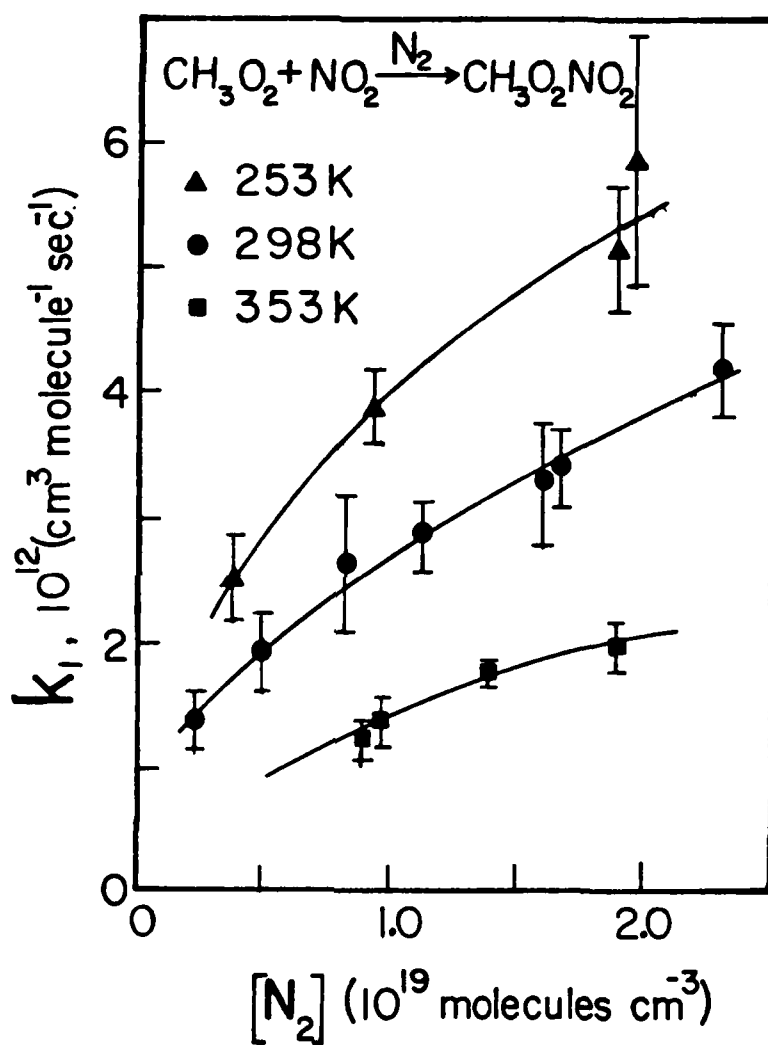| Temperature K	Pressure torr	Number Density 10^{19} molecules cm^{-3}	$k_1 \times 10^{12}$ cm^3 molecule^{-1}s^{-1}
298	76	0.246	1.36 ± 0.23
	157	0.509	1.90 ± 0.32
	258	0.836	2.60 ± 0.56
	352	1.141	2.82 ± 0.28
	500	1.620	3.25 ± 0.50
	519	1.682	3.36 ± 0.32
	722	2.339	4.12 ± 0.38
353	330	0.903	1.19 ± 0.15
	354	0.966	1.35 ± 0.21
	511	1.398	1.71 ± 0.10
	696	1.904	1.93 ± 0.20
253	109	0.416	2.50 ± 0.34
	250	0.954	3.85 ± 0.30
	503	1.920	5.10 ± 0.50
	519	1.981	5.8 ± 1.0

Figure 4. Plots of k_1 vs. N_2 Number Density. The lines drawn through the points are visual best fits.

There are two possible chemical complications that can arise in our experiments: (a) production of O_3 due to reaction of $O(^3P)$ (formed by either O_2 or NO_2 photolysis) with O_2 and (b) production of NO and its subsequent reaction with CH_3O_2. Photolysis of O_2 under the most unfavorable conditions, i.e., high $[O_2](\sim 5 \times 10^{17}$ cm$^{-3})$ and high photolysis laser energy (~ 10 mJ/cm^2), would produce $\sim 1 \times 10^{13}$ $O(^3P)$ cm^{-3}. (The absorption cross section for O_2 at 193 nm is $\sim 1 \times 10^{-21}$ cm^2.[13]) Similary, photolysis of NO_2 would lead to $\sim 1 \times 10^{13}$ $O(^3P)$ cm^{-3}. (The absorption cross section for NO_2 at 193 nm is $\sim 6 \times 10^{-19}$ cm^2[15].) Any $O(^1D)$ that is formed via photolysis would be quenched to $O(^3P)$ in less than 0.1 μsec by N_2.[16] The photolytically produced $O(^3P)$ would then react with either O_2 or NO_2,

$$O(^3P) + O_2 + M \xrightarrow{k_4} O_3 + M \tag{4}$$

$$O(^3P) + NO_2 \xrightarrow{k_5} NO + O_2 \tag{5}$$

The fraction of $O(^3P)$ that would lead to O_3 formation would, of course, depend on the ratio of $k_4[O_2][M]$ to $k_5[NO_2]$. Under the extreme conditions of low temperature (where k_4 is large) and low NO_2, we would produce $\sim 4 \times 10^{12}$ O_3 cm^{-3}. In our experiment, then, we would obtain $\sim 3\%$ absorption of 257 nm radiation due to O_3. However, the O_3 formation does not affect measurement of the CH_3O_2 decay since all O_3 is formed within 100 μsec (99% completion) after the laser flash, and, therefore simply changes the value of I_0. The concentration of O_3 formed is too low to have any effect on the kinetics of the measured rate of CH_3O_2 decay. This conclusion was checked by increasing the photolysis energy by a factor of 4 while keeping $[CH_3O_2]_0$ constant (by decreasing [azomethane] by a factor

of 4); the measured decay rates were, within experimental error, unaffected.

The mount of NO that is produced via NO_2 photolysis would be at most 1.2% when 10 mJ/cm^2 is used for photolysis and all $O(^3P)$ that is produced reacts with NO_2 to produce NO. NO would of course, react with CH_3O_2 to produce CH_3O and NO_2,

$$CH_3O_2 + NO \xrightarrow{k_2} CH_3O + NO_2 \ . \tag{2}$$

The rate constant for Reaction (2) is known to be $\sim 8 \times 10^{-12}$ cm^3 molecule^{-1}s^{-1}.[1-3] Since the measured values of k_1 vary from 1.19 to 5.8×10^{-12} cm^{3}molecule^{-1}s^{-1}, the contribution of Reaction (2) could never be greater than 8% (i.e., at high temperature and low pressures). Again, this possibility was discarded as inconsequentialy by the observation that the measured rate constant was independent of photolysis energy. CH_3O formed in Reaction (2) would react with NO_2 to give CH_3ONO_2.

$$CH_3O + NO_2 \longrightarrow CH_3ONO_2 \ . \tag{6}$$

Formation of CH_3ONO_2 would not affect the measured rate constant since CH_3ONO_2 does not regenerate CH_3O_2, does not strongly absorb 257 nm radiation, and its concentration is too low to effectively remove CH_3O_2 via reaction. (The absorption cross section for CH_3ONO_2 is $\sim 4 \times 10^{-20}$ cm^2 at 257 nm.[17])

In addition to the two photolysis related problems that were discussed above, it is possible that our measured rate constants are incorrect if the thermal decomposition of the $CH_3O_2NO_2$ product leads to CH_3O_2 production on the same time scale as the measured CH_3O_2 decay,

$$CH_3O_2NO_2 \xrightarrow{\text{M}} CH_3O_2 + NO_2 \ . \tag{8}$$

Reaction (7) would, of course, be most severe at higher temperatures. The rate constant for Reaction (7) is not known. However, it cannot be very different from that of HO_2NO_2 decomposition leading to HO_2 and NO_2 production, which has been measured.[18] Using this rate constant, the fastest rate for Reaction (7) at 353K, would be $\sim 20s^{-1}$. This rate is negligible when compared to the $[CH_3O_2]$ decay rates of 699-8837 s^{-1} that were measured at 353K. Experimentally, if Reaction (7) was important, we would have observed non-exponential $[CH_3O_2]$ decays and more importantly, a non-linear dependence of k_1' on $[NO_2]$. We found the $[CH_3O_2]$ to decay exponentially for at least 3 1/e times and k_1' vs $[NO_2]$ plots were linear. Therefore, Reaction (7) could not have been significant under our experimental conditions.

Discussion

There are three separate direct measurements of k_1 at 298K. Cox and Tyndall[9] measured k_1 to be $(1.2 \pm 0.3) \times 10^{-12}$ $cm^3 molecule^{-1} s^{-1}$ at 500 torr of Ar + CH_4, and $k_1 = (1.6 \pm 0.3) \times 10^{-12}$ $cm^3 molecule^{-1} s^{-1}$ at 540 torr N_2, using the molecular modulation technique. This pressure independent value of k_1 is in good agreement with those obtained by Adachi and Basco[10] who measured k_1 to be $(1.53 \pm 0.07) \times 10^{-12}$ $cm^3 molecule^{-1} s^{-1}$ independent of pressure (between 53 and 580 torr Ar) using the method of flash photolysis-kinetic spectroscopy. This pressure independent behavior has been interpreted to mean that Reaction (1) is at its high pressure limit above $\sim$ 50 torr of Ar. Sander and Watson,[2] however, found k_1 to vary from $(1.5 \pm 0.10) \times 10^{-12}$ $cm^3 molecule^{-1} s^{-1}$ at 50 torr N_2 to $(3.94 \pm 0.17) \times 10^{-12}$ $cm^3 molecule^{-1} s^{-1}$ at 700 torr of N_2 at 298K. Moreover, the value of k_1 was observed to be dependent on the nature of the bath gas, i.e., He, N_2, or SF_6. This type of pressure dependent behavior is typical of an addition reaction. Sander and Watson's data also shows that Reaction (1) is in the "fall-off" regime, i.e., between second and third order, in pressure range of 50 to 700 torr of He, N_2, and SF_6. It should also be pointed out that the lower pressure values of k_1 obtained by Sander and Watson agree reasonably well with k_1 values of both Cox and Tyndall, and Adachi and Basco.

As seen from Table III, our measured values of k_1 are in excellent agreement with those of Sander and Watson; this argues very heavily for k_1 being pressure dependent. Sander and Watson have pointed out that the possible reason for the discrepancy between their values at higher pressures and those of Cox and Tyndall, is the long residence time of the gas mixtures and depletion of NO_2 along the length of the cell in

Table III. Comparison of Our Results With Previous Data at 298K.

k_1, $10^{12} \times cm^3 molecule^{-1} s^{-1}$

Pressure torr	Diluent	This Work	Sander and Watson[*] Ref (2)	Cox and Tyndall Ref (9)	Adachi and Basco Ref (10)
50	N_2		1.15±0.10		
76	N_2	1.36±0.23			
100	N_2		1.58±0.15		
157	N_2	1.90±0.32			
225	N_2		2.22±0.31		
258	N_2	2.60±0.56			
350	N_2		2.98±0.23		
352	N_2	2.82±0.28			
500	N_2	3.25±0.50	3.67±0.21		
519	N_2	3.36±0.32			
540	N_2			1.6±0.3	
700	N_2		3.94 ± 0.17		
722	N_2	4.12±0.38			
50	Ar+CH₄			1.2±0.3	
53-580	Ar				1.53±0.07

[*] The preferred value reported by Watson and Sander is the average value $\equiv k_1'/[NO_2]$.

the molecular modulation apparatus. In Adachi and Basco's experiments, the concentrations of reactants used were extremely large. This should have led to many secondary reaction complications. Also, their CH_3O_2 radical detection scheme was quite insensitive. Furthermore, as the authors pointed out, they would have to make a large correction to their high flash energy results due to the participation of Reaction (6), if $k_6 \simeq 8 \times 10^{-12}$ $cm^3 molecule^{-1} s^{-1}$. To date, three separate direct measurements of k_6 have been carried out which yield a value of $k_6 = (8 \pm 2) \times 10^{-12}$ $cm^3 molecule^{-1} s^{-1}$.[1-3] Even though Adachi and Basco carried out a separate set of experiments using low flash energies and obtained values of k_1 (supposedly in the absence of secondary reaction complications) in agreement with their previous measurements, their results have to be considered suspect. They had very large concentrations of free radicals even in their low flash energy experiments which could lead to erroneous results. We believe that at 298K, the data obtained by Sander and Watson and in the present investigation are devoid of secondary reaction complications and hence should be used for atmospheric modeling studies.

There are no previous determinations of the temperature dependence of k_1. Our results are consistant with what is to be expected for an addition reaction which goes through an energy-rich complex. The strong temperature dependence of the measured values of k_1 suggests that $k_{1\infty}$ is likely to be $> 1 \times 10^{-11}$ $cm^3 molecule^{-1} s^{-1}$ at 253K. At 600 Torr, for example, the apparent "activation energy" for Reaction (6) is $\sim$ -1.8 Kcal/mole.

For atmospheric modelling purposes it is convenient to obtain an analytical expression which best describes the temperature and pressure dependence of k_1. Sander and Watson have fit their data for k_1 at 298K

to the following semi-empirical equation which is based on Troe's formulation of RRKM theory:[19]

$$k([M],T) = \frac{k_0(T)[M]}{1 + \frac{k_0(T)[M]}{k_\infty(T)}} \; F_c \; \{1 + [\log_{10}(k_0(T)[M]/k_\infty(T))]^2\}^{-1} \quad (I)$$

$$k_0(T) = k_0(298)\left(\frac{T}{298}\right)^{-n}$$

$$k_\infty(T) = k_\infty(298)\left(\frac{T}{298}\right)^{-m}.$$

In Equation (I), $k_0(k_\infty)$ are the rate constants in the low (high) pressure limits and F_c is a parameter which relates the energy dependence of the rate constant for activated complex decomposition to the shape of the k vs $[M]$ curve. They obtain $k_0(298) = (2.33 \pm 0.8) \times 10^{-30}$ cm^6 molecule^{-1}sec^{-1}, $k_\infty = (7.0 \pm 1.0) \times 10^{-12}$ cm^3 molecule^1 sec^1 and $F_c = 0.4$. Because Sander and Watson's data base at 298K is much larger than ours and because our results are in excellent agreement with theirs, we have fit our temperature dependent data by trial and error with the constraint that $k_0(298)$, $k_\infty(298)$, and F_c must fall within the error limits given by Sander and Watson. The best fit to the data is obtained for (Figure 4)

$$k_0(T) = 2.2 \times 10^{-30} \left(\frac{T}{298}\right)^{-2.5} \text{cm}^6\text{molecule}^{-2}\text{s}^{-1}$$

$$k_\infty(T) = 7 \times 10^{-12} \left(\frac{T}{298}\right)^{-3.5} \text{cm}^3\text{molecule}^{-1}\text{s}^{-1}$$

$$F_c = 0.4 .$$

Our results suggest that Reaction (1) could contribute significantly towards removal of CH_3O_2 and NO_2 in the presence of high concentrations of NO_x (such as those encountered in urban smog) if $CH_3O_2NO_2$ is thermally stable.

25

References

1. I.C. Plumb, K.R. Ryan, J.R. Steven, and M.F.R. Mulcahy, Chem. Phys. Letters $\underline{63}$, 255 (1979).

2. S.P. Sander and R.T. Watson, J. Phys. Chem. (in press).

3. A.R. Ravishankara, F.L. Eisele, and P.H. Wine, presented at the Gordon Conference on Environmental Chemistry—Air, 1979.

4.(a) C.J. Howard and K.M. Evenson, Geophys. Res. Lett. $\underline{4}$, 437 (1977).

  (b) B.Reimann and F. Kaufman, paper presented at 13th Informal Conference on Photochem., Clearwater Beach, FL (1978).

  (c) J.P. Burrows, D.I. Clift, G.W. Harris, B.A. Thrush, and J.P. Wilkinson, W.M.O. Sym. Ozone, Toronto, Canada (1978).

  (d) J.J. Margitan and J.G. Anderson, paper presented at 13th Informal Conference on Photochemistry, Clearwater Beach, FL (1978).

  (e) M.T. Leu, J. Chem. Phys. $\underline{70}$, 1662 (1979).

5. C.J. Howard, J. Chem. Phys. $\underline{71}$, 2352 (1979).

6.(a) C.W. Spicer, A. Villa, H.A. Wiebe, and J. Heicklen, J. Amer. Chem. Soc. $\underline{95}$, 13 (1973).

  (b) R. Simonaitis and J. Heicklen, J. Phys. Chem. $\underline{78}$, 2417 (1974).

  (c) R. Simonaitis and J. Heicklen, J. Phys. Chem. $\underline{79}$, 298 (1975).

7. C.T. Pate, B.J. Finlyason, and J.N. Pitts, Jr., J. Amer. Chem. Soc. $\underline{96}$, 6554 (1974).

8. R.A. Cox, R.G. Derwent, P.M. Holt, and J.A. Kerr, J.C.S. Faraday I, $\underline{72}$, 2444 (1976).

9. R.A. Cox and G.S. Tyndall, Chem. Phys. Lett. $\underline{65}$, 357 (1979).

10. H. Adachi and N. Basco. Int. J. Chem. Kinet. $\underline{XII}$, 1 (1980).

11. P.H. Wine, N.M. Kreutter, and A.R. Ravishankara, J. Phys. Chem. 83, 3191 (1979).

12. A.M. Bass, A.E. Ledford, Jr., and A.H. Laufer, J. Res. Natl. Bur. Stand. Section A $\underline{80}$, 143 (1976).

13. J.G. Calvert and J.N. Pitts, Jr., "Photochemistry," John Wiley and Son, Inc. 1966.

14. S.P. Sander and R.T. Watson, Private communications, 1980.

15. H.S. Johnston, S.G. Chang, and G. Whitten $\underline{78}$, 1 (1974).

16. NASA Reference Publication 1049, "The Strantosphere: Present and Future," Editors, R.D. Hudson and E.I. Reed, (1979).

17. W.D. Taulor, T.D. Allston, M.J. Moscato, G.B. Fazekas, R. Kozlosi, and G.A. Takacs, Int. J. Chemical Kinetics, in press, 1980, and references therein.

18. R.A. Graham, A.M. Winer, and J.N. Potts, Jr., J. Chem. Phys. $\underline{68}$, 4505 (1978).

19. J. Troe, J. Phys. Chem. $\underline{83}$, 114 (1979).
    J. Troe, J. Chem. Phys. $\underline{66}$, 4758 (1977).

Acknowledgements

APPENDIX I

Preparation of Azomethane

The apparatus used for preparation of azomethane is shown in
Figure 1a. The method we used is a slightly modified version of the
Renaud and Leitch preparation procedure.

Ten grams of Sym-1,2-dimethylhydrazinedihydrochloride (obtained from
Aldrich Chemical Co.) was slowly added to 25 ml of 6N NaOH contained in
a 250 ml Erlenmeyer flask. The flask was cooled in an ice bath and the
contents vigorously stirred using a magnetic stirrer. When 10 gm of Sym
1,2-dimethylhydrazinedihydrochloride was added, $\sim$ 3 ml of 6N NaOH was
mixed with this solution to dissolve any remaining solid. This solution
was transferred to the dropping funnel.

35 grams of mercury (II) oxide was mixed with 50 ml of distilled
water in the three-necked 500 ml flat-bottom flask. The three-necked
flask was connected on one side to a helium tank and another side to a
cold finger. The cold finger, maintained at 0°C with crushed ice, was
connected to two glass traps in series. Both traps were cleaned by
flaming them under vacuum.

Before starting the addition of the solution present in the dropping
funnel to the three-necked flask, the assembled system was flushed with
He for at least one hour to remove all traces of air present in the
assembly. The first trap was maintained at 193K (dry ice—trichloro-
ethylene slush) and the second at $\sim$ 163K (ethanol cooled with liquid N_2).
The solution in the dropping funnel was added in drops to the slurry of
mercuric oxide which was slowly stirred with a magnetic stirrer. The
addition was completed in $\sim$ 45 minutes and He allowed to flow for another
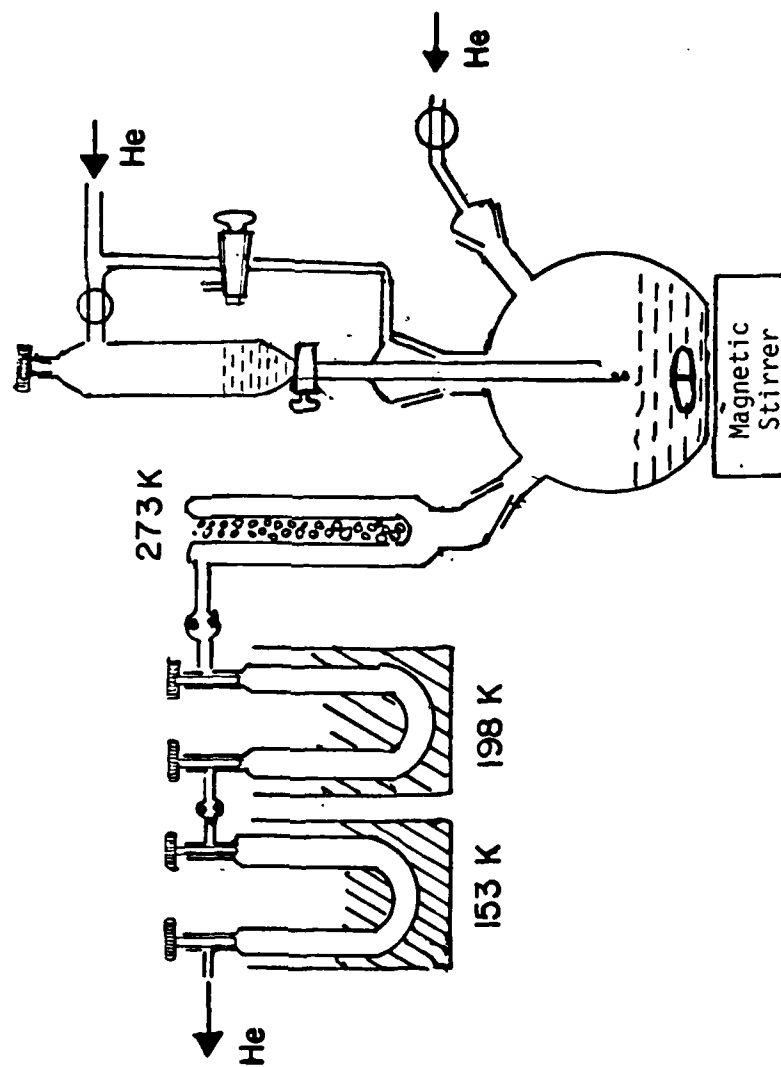
29

Figure 1a. Apparatus for the Preparation of Azomethane.

20 minutes to sweep out any remaining azomethane in to the traps. (The flow rate of helium was ∿ 20 ml/min.)

The traps were disconnected from the assembly and cooled to 77K with liquid N_2 to pump out He before transferring the contents to a bulb. The cold finger of the bulb was then maintained at 197K and azomethane distilled into a storage vessel maintained at 77K. The first and the last fractions were discarded. The vapor pressure of azomethane at 197K is ∿ 7 torr while that of H_2O is less than 1×10^{-3} torr which enabled us to separate the two.

All preparation and handling of azomethane was carried out in the dark or under red lights to avoid photolysis. The azomethane was stored at 197K.

APPENDIX II

Generation of the 257 nm CW UV Laser Beam

A schematic diagram of the setup is shown in Figure 2a. A Lexel model 95 Argon ion laser was operated on the 514 nm line. The out of this laser was checked to ensure that the laser was operating in TEM_{00} mode. The Gaussian beam was focused using a 10 cm focal length quartz plano convex lens to obtain a tight beam waist with a confocal parameter of 10 cm. (The focal length at 514 nm of the lens was accurately measured using the cat's eye technique) The position of the lens was adjusted to locate the beam waist in the middle of a 50 mm long (10 mm x 10 mm on the side) ADP crystal (Inrad Corp.) which was housed in a gold plated copper block. This copper block was in snug contact with a gold plated pedestal which was backed by a Paltier thermoelectric cooler. The Peltier cooler itself was backed by a heater block which, in turn, was cooled by circulating water at a constant temperature ($\pm$ 2 °C) from a temperature controlled five gallon water bath heated by a fish tank heater. By adjusting the rate of water flow and the temperature of the heater block (which was controlled by a proportional heater) the temperature of the ADP crystal could be maintained at -10 °C with a precision of $\pm$ 0.1 °C. We found that the doubled 257 nm output was a maximum at this temperature.

The 257 nm beam was diverging as it exited the crystal; this beam was rendered parallel by a second lens ($\sim$ 15 cm focal length at 257 nm). The collinear 257 nm and 514 nm beams were dispersed by a prism and the 514 nm beam stopped by a block. The entire assembly was housed inside a box to prevent dust from getting in and 514 nm light from scattering out.
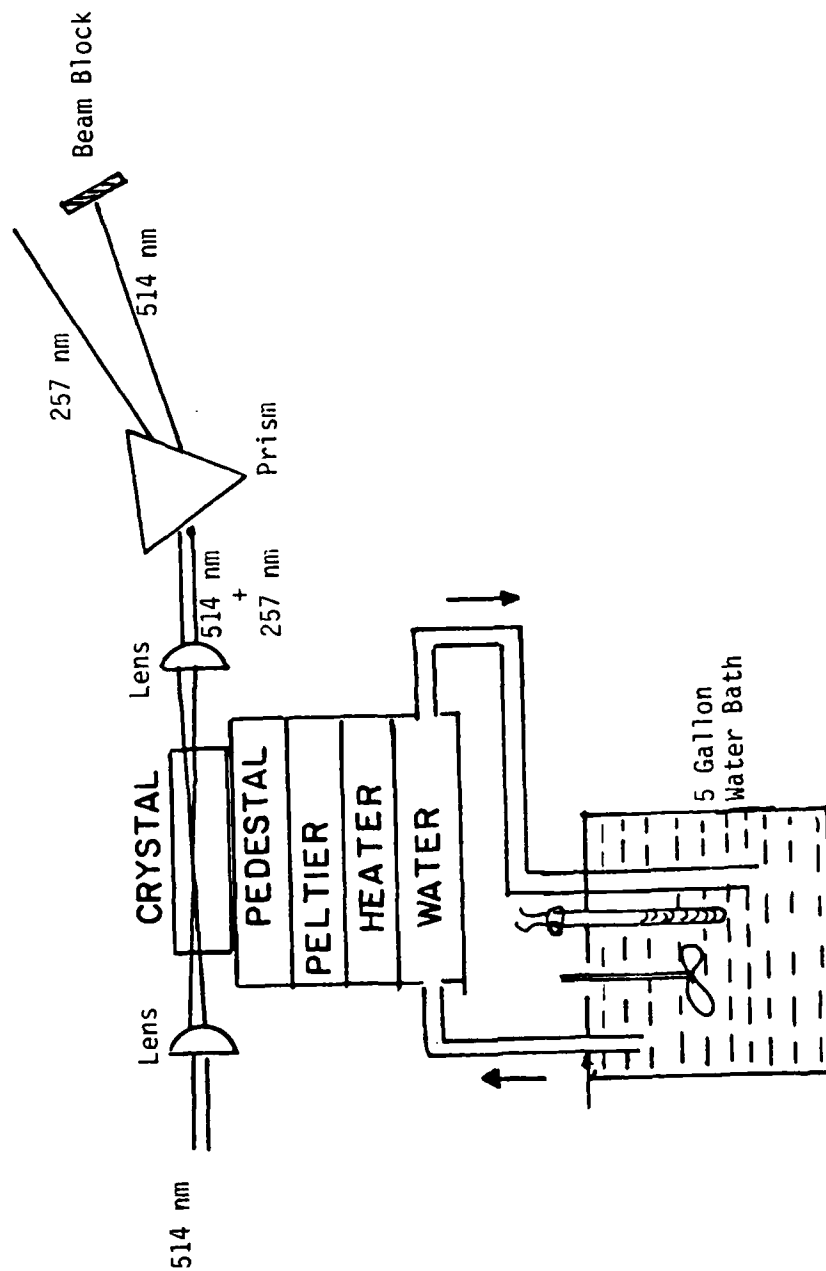
Figure 2a. Details of the Second Harmonic Generation Set Up.

With an input energy of 1 W at 514 nm, we could routinely obtain $\sim 50\,\mu W$ of 257 nm, which was more than adequate to carry out our experiments.

2-8